

## Article

# Landslide Susceptibility Assessment in Nepal's Chure Region: A Geospatial Analysis

Purna Bahadur Thapa<sup>1</sup>, Saurav Lamichhane<sup>2,\*</sup>, Khagendra Prasad Joshi<sup>3</sup> , Aayoush Raj Regmi<sup>4</sup> ,  
Divya Bhattarai<sup>5</sup> and Hari Adhikari<sup>6,\*</sup> 

<sup>1</sup> Institute of Forestry, Hetauda Campus, Tribhuvan University, Hetauda 44100, Nepal

<sup>2</sup> Faculty of Forestry, Agriculture and Forestry University, Hetauda 44100, Nepal

<sup>3</sup> Kathmandu Forestry College, Tribhuvan University, Kathmandu 44600, Nepal

<sup>4</sup> School of Forestry & NRM, Institute of Forestry, Tribhuvan University, Kathmandu 44600, Nepal

<sup>5</sup> Institute of Botany and Landscape Ecology, University of Greifswald, Soldmannstraße 15, 17489 Greifswald, Germany

<sup>6</sup> Department of Geosciences and Geography, University of Helsinki, P.O. Box 64, FI-00014 Helsinki, Finland

\* Correspondence: sauravlc8@gmail.com (S.L.); hari.adhikari@helsinki.fi (H.A.)

**Abstract:** The Chure Hills, already vulnerable due to their fragile nature, face increased landslide risk, prompting the need for reliable susceptibility assessment. This study uses Poisson regression modeling to assess landslide susceptibility in two highly susceptible districts of the Chure region. Variance inflation factor (VIF) tests were conducted to ensure robustness, indicating no multicollinearity among the variables. Subsequently, Poisson regression analysis identified eight significant variables, among which geology, lineament density, elevation, relief, slope, rainfall, solar radiance, and land cover types emerged as important factors associated with landslide count. The analysis revealed that higher lineament density and slope were associated with lower landslide counts, indicating potential stabilizing geological and topographical influences. The categorical variable, namely geology, revealed that middle Siwalik, upper Siwalik, and quaternary geological formations were associated with lower landslide counts than lower Siwalik. Land cover types, including areas under forest, shrubland, grassland, agricultural land, water bodies, and bare ground, had a substantial significant positive association with landslide count. The generated susceptibility map that exhibited a substantial portion (23.32% in Dang and 5.22% in Surkhet) of the study area fell within the very-high-susceptibility categories, indicating pronounced landslide susceptibility in the Dang and Surkhet districts of the Chure hills. This study offers valuable insights into landslide vulnerability in the Chure region, serving as a foundation for informed decision-making, disaster risk reduction strategies, and sustainable land-use and developmental policy planning.



**Citation:** Thapa, P.B.; Lamichhane, S.; Joshi, K.P.; Regmi, A.R.; Bhattarai, D.; Adhikari, H. Landslide Susceptibility Assessment in Nepal's Chure Region: A Geospatial Analysis. *Land* **2023**, *12*, 2186. <https://doi.org/10.3390/land12122186>

Academic Editors: Raffaele Pelorosso, Andrea Petroselli, Matej Vojtek and Hariklia D. Skilodimou

Received: 19 October 2023

Revised: 7 December 2023

Accepted: 15 December 2023

Published: 18 December 2023



**Copyright:** © 2023 by the authors. Licensee MDPI, Basel, Switzerland. This article is an open access article distributed under the terms and conditions of the Creative Commons Attribution (CC BY) license (<https://creativecommons.org/licenses/by/4.0/>).

**Keywords:** landslide susceptibility; Chure region; poisson regression; susceptibility map

## 1. Introduction

Landslides, a significant geo-hazard, have profound implications worldwide, causing substantial loss of life, damage to infrastructure, and environmental degradation [1,2]. Nepal, nestled in the Himalayas, faces significant landslide challenges due to its rugged terrain and complex geology, causing substantial economic and human loss [3]. One region particularly susceptible to landslides is the Chure region of Nepal, located in the southern foothills of the Himalayas. The Chure region's unique topography, geological composition, and anthropogenic activities contribute to its heightened vulnerability to slope failure and landslides [4]. Understanding the causes and impacts of landslides in this region is crucial for effective susceptibility assessment, mitigation, and sustainable development.

The Chure region of Nepal has key ecological and socioeconomic significance. It is one of the country's major carbon reservoirs, is rich in biodiversity, possesses high-value

timber species, and is the efficient water supply source for the Terai region of the country [5]. Nearly four million populations from the Chure and Bhabhar regions depend on the site's local natural resources to generate livelihoods and income [6]. Despite its broad ecological and socioeconomic significance, it faces substantial outside challenges. The environment of the Chure region is undergoing unprecedented changes through illegal logging, uncontrolled mining, and increased anthropogenic activities [7]. The other activities contributing to the loss of its environmental assets are over-exploitation of natural resources, free livestock grazing, and the illegal trade in forest products [8]. The region is delicate and environmentally sensitive due to the composition of loose materials that are derived from soft rocks [6]. Foreseeing its threat and considering its significance, the Government of Nepal created the President Chure Terai Madesh Conservation Development Board in 2010 to conserve and manage the region's land, water, and forest for ecological stability in the region [9].

Technological advancements and data analysis tools have recently revolutionized our understanding of landslides. Google Earth data, geographic information systems (GIS), remote sensing, and modeling techniques have become indispensable for studying landslide dynamics and assessing their potential risks [10–12]. Google Earth's high-resolution satellite imagery provides valuable visual information, enabling researchers to identify landslide-prone areas and study their geomorphological characteristics [13]. GIS facilitates the integration and analysis of diverse spatial datasets, aiding in identifying the factors contributing to landslide occurrences [14]. Furthermore, freely available high-resolution data, such as the digital elevation models, have aided in precisely mapping terrain features and monitoring landslide activity [15,16].

There are two major approaches in the landslide susceptibility assessment: qualitative and quantitative methods. Qualitative methods are inventory-based and knowledge-driven, whereas quantitative methods are data-driven and physically based models [17]. According to its occurrence data, the qualitative methods classify areas with similar geomorphological and lithological properties, ultimately indicating the region that is highly susceptible to landslides [18]. On the other hand, the quantitative methods include statistical, probabilistic, artificial intelligence-based, and deterministic approaches [19,20]. The quantitative approach is more reliable as this technique's prediction of landslide susceptibility is based on actual data and interpretations [21,22]. Many techniques, such as statistical tools [23,24], frequency ratios [25,26], the weight of evidence [27], and the analytical hierarchical process [21,28], are used by many researchers to produce precise results with reasonable accuracy for landslide assessment. Among the various approaches, the generalized linear model (GLM) is one of the most common statistical methods for landslide prediction modeling [29]. GLMs offer greater flexibility in analyzing relationships among variables because they can handle a wide range of continuous and categorical data [30].

Landslides occur at unexpected sites and uncertain times; thus, they are called stochastic processes. These stochastic processes are often modeled using a probability-based approach. The Poisson model, a mathematical framework that operates in a continuous time and consists of random point-events (landslide) in ordinary time, which is treated as a continuous and uninterrupted flow, is used for the calculation of the occurrence of random point-events in time and is used commonly to model the occurrence of landslides [31,32]. Geographic information systems (GIS) have been found to play beneficial roles in the study of landslides since they combine the functions of data collection, storage, manipulation, display, and analysis with a spatial framework. Integrating GIS and multivariate statistics is a fruitful approach in landslide mapping [14,33]. Previously, many studies have used GIS and other evaluation techniques (frequency ratio, logistic regression method) for landslide hazard assessments [34,35]. However, limited research has been conducted focusing specifically on the Chure Hills for landslide susceptibility and factors influencing it. Thus, this study attempts to explore the application of the Poisson model and GLM, as it is mainly based on actual data, requires less theoretical data, and enables the researchers and policymakers to gain crucial insights into landslide dynamics and preparedness measures

and develop sustainable land management strategies in similar geographical regions of Nepal. Such comprehensive approaches will be instrumental to mitigating landslide risks and fostering resilient communities in this vulnerable region.

## 2. Study Area

The Chure range of Nepal is a long strip spanning from its western to its eastern boundary (Figure 1). It constitutes almost 26% of the total population of Nepal across 37 districts [36]. The Chure range accounts for 12.78% of the country's land area, containing 14 forest ecosystems [37]. Climate-wise, the Chure range mainly falls under temperate regions with an elevation of 120–2000 m, a temperature of 15.8–31.8 °C, and precipitation between 1400 and 2000 mm per year [6,9]. The region is very young and geologically composed of loose and soft rocks, which are very vulnerable to sedimentation during peak monsoon due to a high number of gullies [4,6]. The physiography of the Chure range can be divided into the main Chure hillslopes, the Bhawar Dun valleys, and the inner river valley [38]. Among these different physiographical divisions of the Chure region, the hills of Chure are in the greatest danger of landslides due to their weak geomorphic structure, very dry summers, and high risk of erosion in monsoon due to the larger number of rivers running throughout the hills [4]. In contrast, the Bhawar region is densely covered with forests [39], reducing landslide risk.

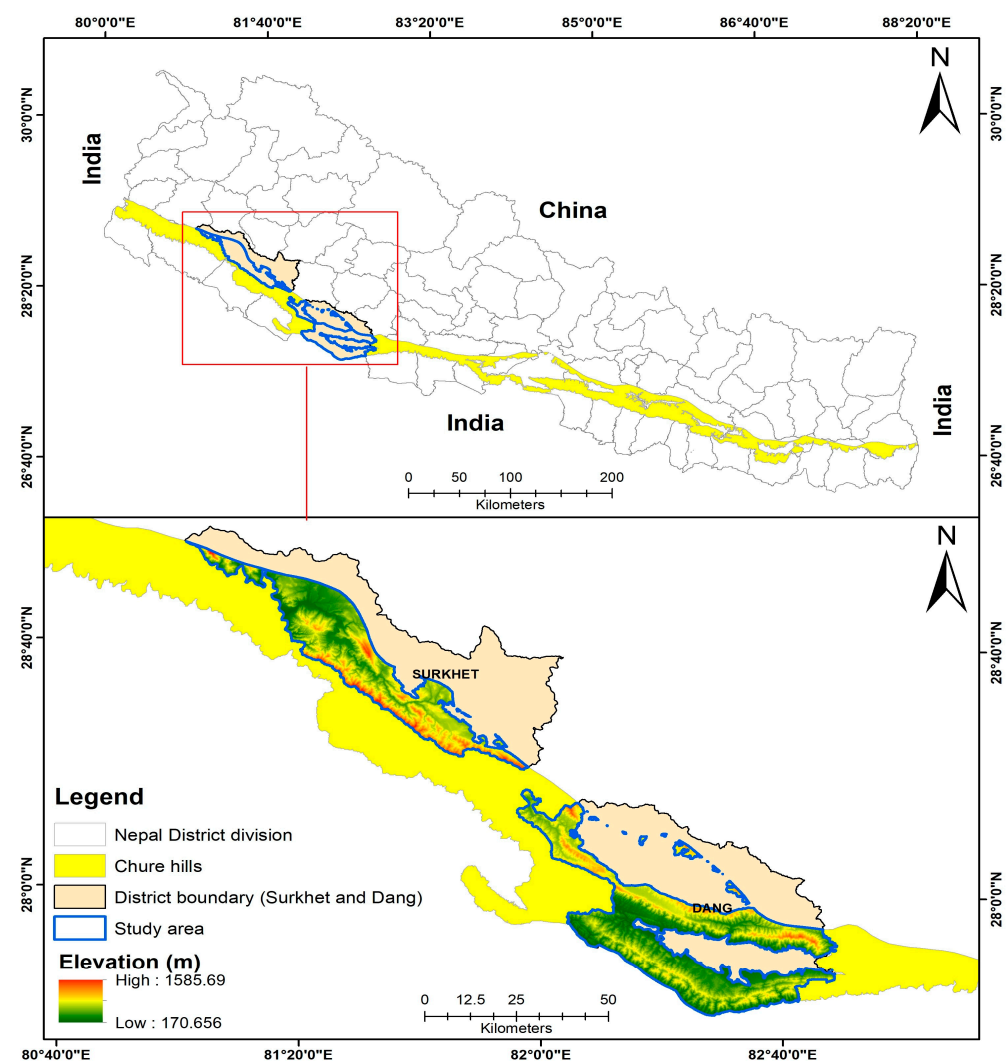


Figure 1. The geographical location of Nepal, along with study area.

Meanwhile, the Dun and the inner river valley are mostly urbanized and agricultural plain areas, which, when building landslide inventory, created a high number of non-occurrence data. This can lead to a misbalance in occurrence and non-occurrence data, leading to biases in predictive modeling [40]. Therefore, we only assessed the Chure Hills area, neglecting the Bhawar and the valleys. The shapefile of the Chure hills in Figure 1 was downloaded from <https://www.chureboard.gov.np/> (accessed on 15 July 2023).

As a case study approach, our analysis focused on two districts, namely Dang and Surkhet. According to Petley et al. [3], population growth, land-use changes, urbanization, and linear infrastructure development are the driving factors of landslides. Therefore, the selection of these districts was made purposively with the following criteria: (1) a high proportion of fragile Chure hills, (2) a high population growth rate, (3) biologically significant areas, (4) land-use changes, and (5) the excavation of sand, gravel, and boulders.

Dang district comprises the largest portion of the Chure Hills, covering around 11% of the total area, making it the largest district in the Chure Hills. Similarly, Surkhet district ranks fifth, encompassing approximately 7% of the Chure Hills region. The total area of Dang along with Surkhet is 5548.44 km<sup>2</sup> (<https://sthanitya.gov.np/gis>, accessed on 20 July 2023), with the Chure hills in the region covering 2577.06 km<sup>2</sup>, which is nearly half of the total area of these two districts in the Chure region. These two districts also have very high population growth rates, with Dang and Surkhet having rates of 1.92% and 1.62%, respectively [36]. These two districts contain rich species diversity and are home to various biologically significant areas. For instance, the Kakrebihar protected forest, ten wetlands in Surkhet, and the Dang–Deukhuri foothills forest, which is a part of the Terai Arc Landscape conservation, are key providers of the livelihoods of local people and harbor various endangered species [37].

Despite their profound importance, the Chure hills in Surkhet and Dang are at high risk of soil erosion, landslides, and river-bank cutting. This risk is mainly due to existing excavation sites—nine in Dang and one in Surkhet—with the potential for a further increase to eight in Dang and four in Surkhet [9]. Furthermore, the increased number of settlements, intense land-use change, encroachment, geology, and many other anthropogenic factors make this region prone to natural hazards, such as landslides and erosion [39].

### 3. Materials and Methods

#### 3.1. Data Collection and Processing

Our methodology integrates advanced remote sensing technology, ArcGIS 10.3 software, manual interpretation, field verification, and statistical modeling to investigate landslides. This study utilized Remote Sensing data from Google Earth™ and applied ArcGIS 10.3 software for interpretation and analysis. Firstly, the landslide inventory was manually created by visually interpreting landslides in Google Earth in 2022. Each landslide-impacted area was clipped into landslide polygons and converted into shape files to enable further processing and analysis within the ArcGIS 10.3 software. Secondly, a comprehensive analysis is needed to determine the distribution and frequency of landslide occurrences using the compiled landslide inventory data. By employing this data-processing approach, we aimed to enhance the effectiveness and accuracy of our study, providing valuable insights into landslides in the specified timeframe. A subset of 10% of the total landslide incidents was verified through direct field observations to validate the occurrence of landslides in the study region (Figure 2). This verification process was conducted to ensure the accuracy of our results. Finally, the analysis for the predictive assessment of the landslide-susceptible area was conducted through a grid-based generalized linear model (GLM). The study area was divided into grids with sizes of 5 × 5 km<sup>2</sup> (i.e., (25 km<sup>2</sup>) grids ( $n = 620$ ) using “Fish net” tools in Arc GIS 10.3. We examined 1279 locations where landslides had occurred, allowing us to derive comprehensive insights for our study.

### 3.2. Factors Influencing Landslides

Landslides, like many natural hazards, result from a combination of various factors rather than a single, specific cause. There is no consensus about which variables give the best outcome for landslide prediction and modeling; rather, various studies have utilized various factors for landslide analysis [18,21,41,42]. In this study of landslide hazard assessments, various factors influencing landslide occurrences were thoroughly examined, analyzing the previous landslide research. Curvature, a key aspect impacting surface runoff and ground infiltration, was found to play a significant role in surface erosion and groundwater conditions [43]. As curvature values become increasingly negative, the likelihood of landslides occurring escalates [43,44]. Elevation, a vital component in landslide susceptibility mapping, also influences environmental conditions on slopes, including human activity, vegetation, soil moisture, and climate [43,45,46]. Past studies have suggested that higher elevations are more prone to landslides than lower elevations [41,47]. The topographical wetness index (TWI) was identified as another significant factor contributing to landslides, as it quantitatively displays terrain control on soil moisture's spatial distribution [43].

Slope angles are directly related to landslide occurrence, where steeper slopes increase the likelihood of landslides [43,48,49]. Drainage density was also positively correlated with erosion, making it a factor responsible for landslide occurrence [50]. Lineament distance, as determined by Lee and Talib [44], was found to influence landslide conditions. Land cover types were shown to have varying impacts on landslides [51–53], and, hence, land cover was incorporated as a significant landslide conditioning factor in this research.

Geology emerged as a factor in accelerating landslides [54,55]. Previous studies highlighted rainfall as another important factor involved in causing landslides [43,56]. Additionally, annual solar radiation, expressed as the mean solar radiation at a specific pixel over a year, significantly influences landslides [47]. Higher solar radiation in certain areas intensifies sunlight, causing increased moisture evaporation from the exposed soil [57]. Consequently, this heightened evaporation can render these areas more susceptible to landslides [58]. Hence, the solar radiation map was created by utilizing the digital elevation model (DEM) using the "Area solar radiation" toolkit in ArcGIS and then converted to  $\text{KWH}/\text{m}^2$  using a raster calculator. The relative relief of the study area, as demonstrated by Singh and Kumar [59], profoundly impacted natural conditions, shaping the susceptibility to landslides. Furthermore, the distance from roads emerged as a crucial parameter affecting landslide occurrence, with road construction activities disrupting natural slopes and rendering areas near the toe more vulnerable and weakened along highways [60]. Incorporating these factors into the study provides valuable insights into the complex interplay between elements influencing landslide hazard assessment. Figure 3 illustrates the comprehensive methodological framework employed in this study.

### 3.3. Data Analysis

The statistical data analysis process involved a series of sequential steps used to comprehensively examine the features of landslide occurrences. Initially, the R Statistical package v4.0.4 [61] was utilized for data analysis. They were systematically divided into groups to enhance the understanding of the assigned predictors, as illustrated in Table 1. Descriptive summaries of landslides were then computed using the Pivot table function in Microsoft Excel 2013. Subsequently, a generalized linear model (GLM) was employed, incorporating 15 independent variables (Figure 4) as predictors with a Poisson error distribution. The GLM, known for its versatile utilization of variables through a link function that accommodates categorical, continuous, and both types of data, was chosen rather than traditional linear regression modeling [30]. Specifically, the Poisson family GLM was utilized in this study, considering the presence and absence of the grid and the frequency of data in each grid.

**Table 1.** Description of the significant variables used in this study.

S.N.	Variables	Type	Unit	Source
1.	Elevation	Continuous	Meter	(LPDAAC, 2019, [62])
2.	Curvature	Continuous	Degrees/m	Delineated from DEM
3.	Drainage density	Continuous	km/km <sup>2</sup>	Delineated from DEM
4.	Lineament	Continuous	km/km <sup>2</sup>	Delineated from DEM
5.	Rainfall	Continuous	Millimeter	(Fick and Hijmans, 2017, [63])
6.	Relief	Continuous	Meter	Delineated from DEM
7.	Slope	Continuous	(°)	Delineated from DEM
8.	Topographical wetness index	Continuous	Unit less	Delineated from DEM
9.	Geology (Lower Siwalik = 0)	Categorical	Unit less	(ICIMOD, 2020, [64])
10.	Area of water bodies	Continuous	m <sup>2</sup>	(ESRI, 2020, [65])
11.	Area under forest	Continuous	m <sup>2</sup>	(ESRI, 2020, [65])
12.	Area of grassland	Continuous	m <sup>2</sup>	(ESRI, 2020, [65])
13.	Area of agricultural land	Continuous	m <sup>2</sup>	(ESRI, 2020, [65])
14.	Area of shrubland	Continuous	m <sup>2</sup>	(ESRI, 2020, [65])
15.	Distance from road	Continuous	Meter	(OCHA Nepal, 2021, [66])
16.	Solar radiance	Continuous	KWh m <sup>-2</sup>	Delineated from DEM

**Figure 2.** Ground verification and Google Earth points: (A) western Side of Chure region of Surkhet district (Location: Kale Khola); (B) eastern side of Chure region of Dang district (Location: Khoreya).

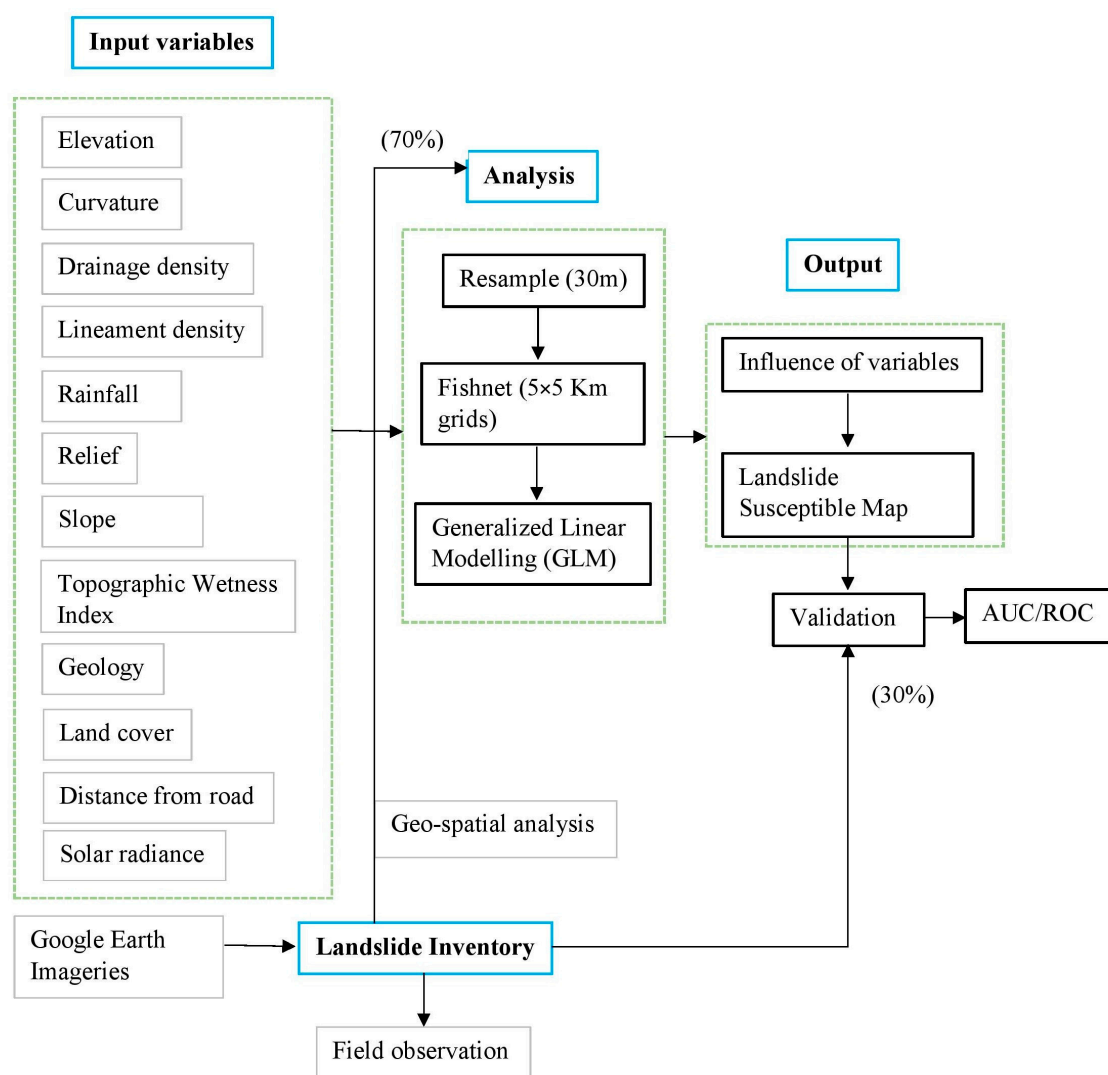


**Figure 3.** Methodological framework of this study.

Once all the variables were finalized and compiled, they were resampled to the same extent and resolution of 30 m for further analysis. This involved clipping the variables to form 30 km<sup>2</sup> cells. Model fitting was performed using the 'DescTools' package [67] and the 'manipulate' package [68]. Prior to constructing the model, a multicollinearity test was conducted using the VIF (variance inflation factor) function from the 'faraway' package [69] for all variables. Importantly, none of the variables exhibited significant multicollinearity (VIF value > 5), thereby allowing the inclusion of all variables in the model construction [70]. Weightage was assigned to each variable based on the coefficient values obtained from the model to predict the potential landslide susceptibility map. ArcGIS 10.8 was then employed to prepare the final landslide susceptibility map. The model's effectiveness was assessed through the AUC curve, ranging between 0 and 1, where a value of 1 is considered the maximum. Models or classifications with an AUC value above 0.9 were regarded as outstanding, those in the range of 0.8–0.9 were regarded as excellent, and those in the range of 0.7–0.8 were regarded as acceptable. Values below 0.5 were considered false and inaccurate [71].

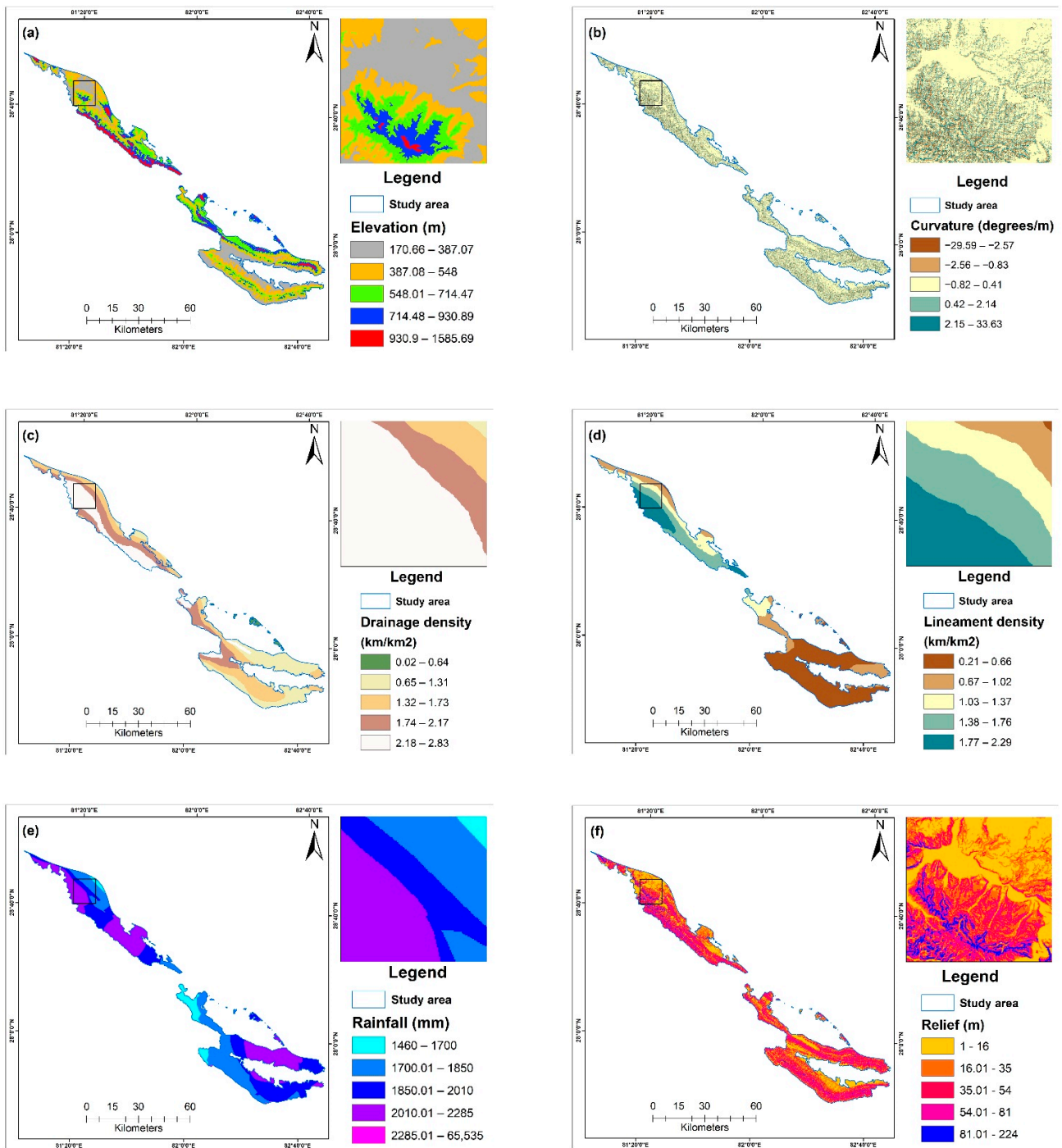
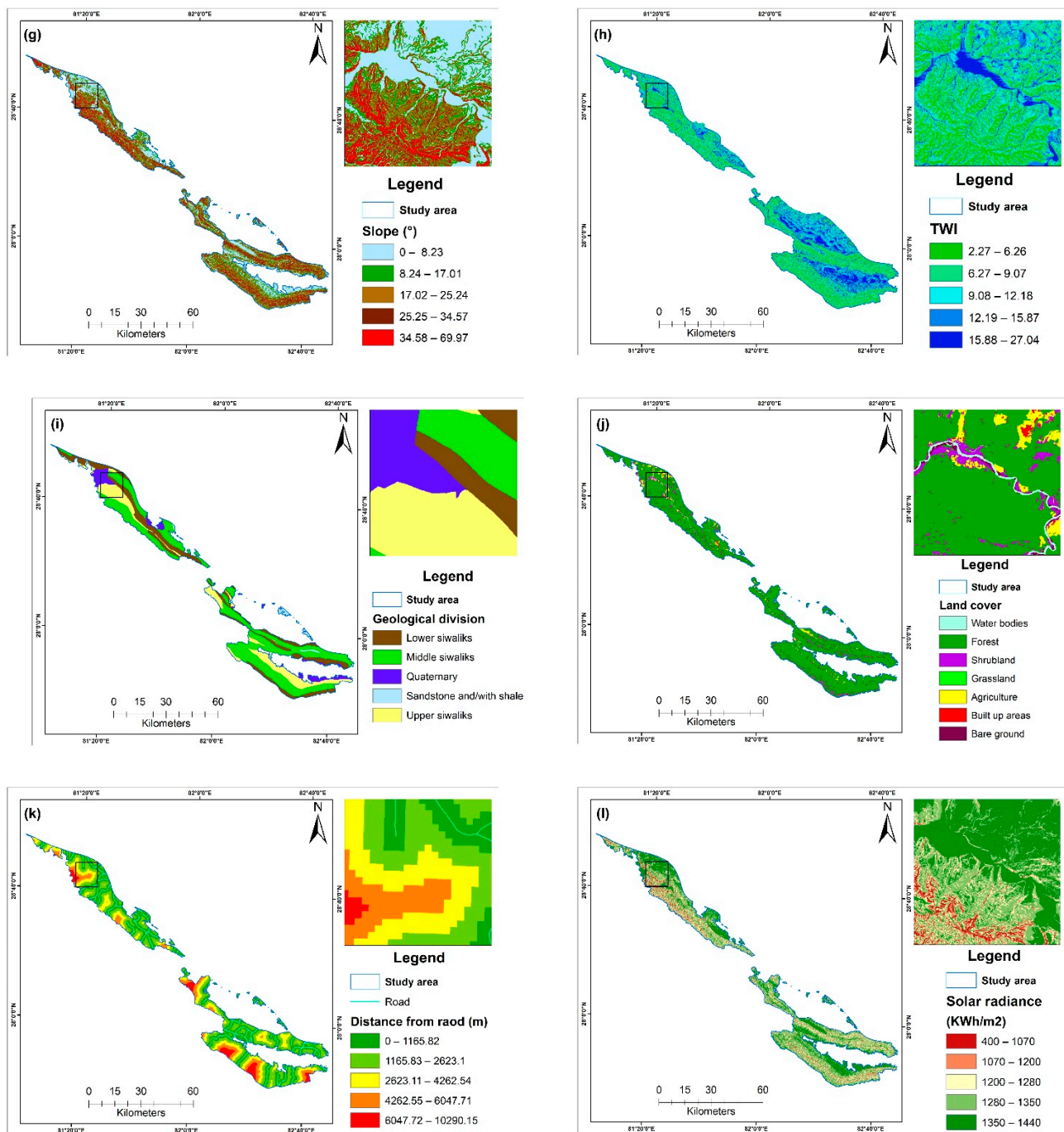


Figure 4. Cont.



**Figure 4.** Predictor variables considered for spatial analysis: (a) elevation, (b) curvature, (c) drainage density, (d) lineament density, (e) rainfall, (f) relief, (g) slope, (h) topographical wetness index (TWI), (i) geology, (j) land cover, (k) distance from road, and (l) solar radiance.

## 4. Results

### 4.1. Geospatial Analysis of Landslide

The spatial analysis of the landslide points was conducted to determine the spatial pattern of landslides across variables. In examining the land cover within the study area, disparities in the distribution of different land cover classes were identified. The forest area emerged as the dominant cover class, constituting approximately 83% ( $n = 1041$ ) of the total landslide count. Shrubland and grassland followed with 15.2% ( $n = 189$ ) and 3%

( $n = 49$ ), respectively. Other land cover types, including water bodies, agricultural areas, and bare ground, collectively accounted for less than 1% of the total landslides.

Concerning the geological divisions, the middle Siwalik region exhibited the highest concentration of landslides, representing approximately 51% of the cases, while the lower Siwalik, upper Siwalik, and quaternary divisions contributed 35% ( $n = 441$ ), 11% ( $n = 142$ ), and 1% ( $n = 22$ ) of the landslides, respectively. Proximity to roads played a crucial role in landslide occurrence, with a notable increase in incidence within 2000 m. Furthermore, areas at altitudes between 300 and 600 m above mean sea level demonstrated the highest incidence of landslides, comprising a significant portion of the total landslides ( $n = 642$ ). The examination of relief, representing elevation variations between points, identified the 50–60 m range as having the highest landslide frequency. Regarding drainage and lineament density, the distribution of landslide data exhibited an uneven pattern. However, the 1–1.5 km/km<sup>2</sup> drainage density range and the above 1.2 km/km<sup>2</sup> lineament density range were associated with the greatest number of landslides, accounting for 54% ( $n = 671$ ) of the cases. Landslides with slopes between 20 and 50 degrees, particularly those with slopes above 35 degrees that are concave in nature, contributed to nearly 64% of landslides ( $n = 539$ ). Furthermore, concerning the climatic variables, it was observed that regions characterized by rainfall exceeding 1800 mm/month exhibited the highest landslide frequency, accounting for a substantial 81% ( $n = 1017$ ) of the recorded cases. Similarly, areas displaying a topographical wetness index (TWI) within the range of 5–10 constituted 53% ( $n = 659$ ), and solar radiance between 1300 and 1350 KWh m<sup>-2</sup> demonstrated elevated landslide occurrence (Figure 5).

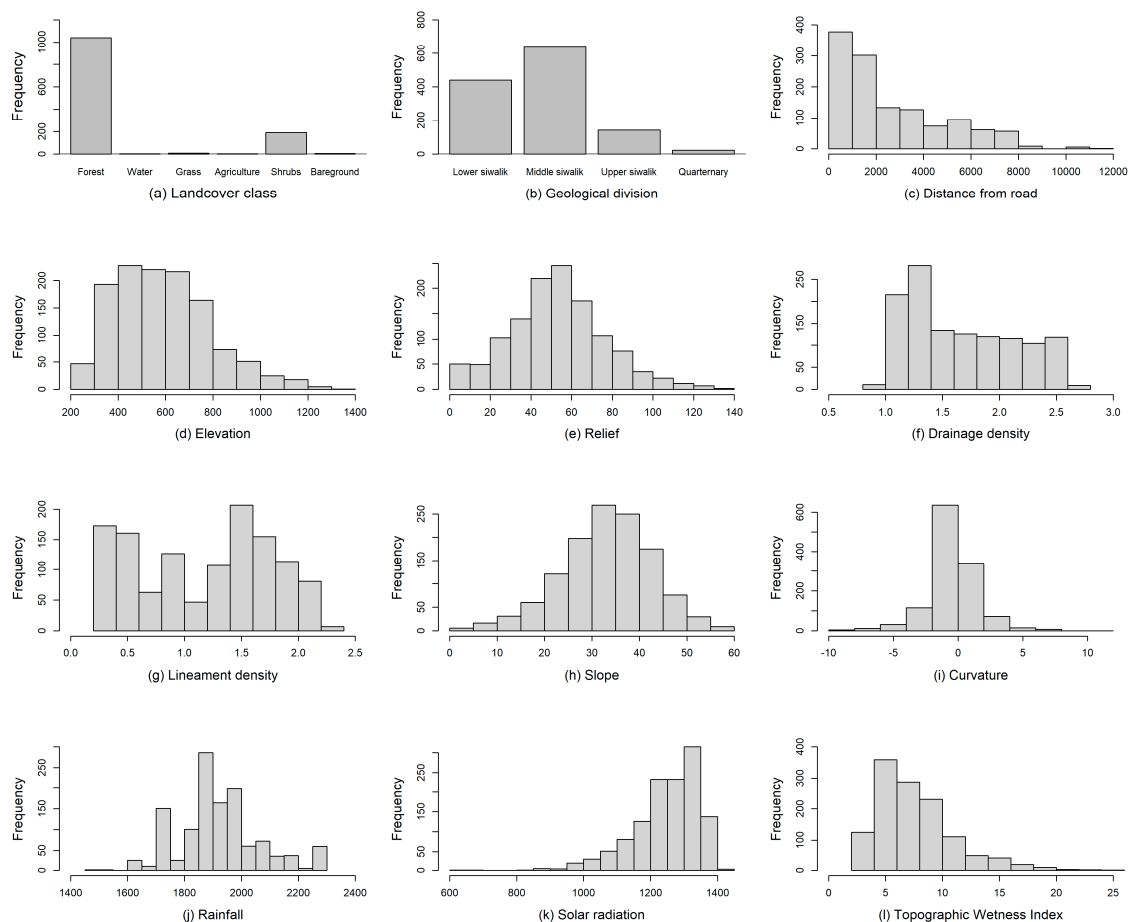


**Figure 5.** Landslide frequency across various variables: (a) land cover, (b) geology, (c) distance from road, (d) elevation, (e) relief, (f) drainage density, (g) lineament density, (h) slope, (i) curvature, (j) rainfall, (k) solar radiation, and (l) topographical wetness index.

### 4.2. Influence of Variables on Landslides

We conducted a comprehensive analysis to understand the factors influencing the occurrence of landslides in the study area. The Poisson regression model that we employed yielded valuable insights into the relationship between landslide count and several environmental variables (Table 2).

**Table 2.** Generalized linear model with the Poisson structure for the probability of landslide occurrence.

	Estimate	Std. Error	z Value	Pr (>  z )
(Intercept)	−5.25	$3.62 \times 10^{-1}$	−14.503	$<2.00 \times 10^{-16}$ ***
Curvature	$-2.07 \times 10^{-2}$	$1.80 \times 10^{-2}$	−1.155	0.248151
Digital elevation model	$1.32 \times 10^{-3}$	$1.91 \times 10^{-4}$	6.903	$5.08 \times 10^{-12}$ ***
Drainage density	$-1.37 \times 10^{-5}$	$4.68 \times 10^{-5}$	−0.292	0.770134
Lineament	$-5.83 \times 10^{-1}$	$8.50 \times 10^{-2}$	−6.86	$6.91 \times 10^{-12}$ ***
Rainfall	$1.46 \times 10^{-3}$	$2.04 \times 10^{-4}$	7.168	$7.63 \times 10^{-13}$ ***
Relief	$6.42 \times 10^{-3}$	$1.93 \times 10^{-3}$	3.324	0.000889 ***
slope	$-1.09 \times 10^{-4}$	$1.90 \times 10^{-5}$	−5.719	$1.07 \times 10^{-8}$ ***
Solar	$2.01 \times 10^{-2}$	$2.80 \times 10^{-3}$	7.171	$7.44 \times 10^{-13}$ ***
Topographical wetness index	$4.31 \times 10^{-4}$	$1.05 \times 10^{-2}$	0.041	0.96737
Middle Siwalik	$-5.94 \times 10^{-1}$	$6.84 \times 10^{-2}$	−8.673	$<2.00 \times 10^{-16}$ ***
Upper Siwalik	−1.20	$1.25 \times 10^{-1}$	−9.636	$<2.00 \times 10^{-16}$ ***
Quaternary	−1.32	$2.66 \times 10^{-1}$	−4.965	$6.87 \times 10^{-7}$ ***
Area of water bodies	$1.24 \times 10^{-6}$	$4.79 \times 10^{-7}$	−2.587	0.009679 **
Area of forest	$2.73 \times 10^{-7}$	$2.72 \times 10^{-8}$	10.03	$<2.00 \times 10^{-16}$ ***
Area of grassland	$2.21 \times 10^{-5}$	$5.07 \times 10^{-6}$	4.35	$1.36 \times 10^{-5}$ ***
Area of agricultural land	$6.63 \times 10^{-7}$	$2.39 \times 10^{-7}$	2.779	0.005454 **
Area of bare ground	$2.08 \times 10^{-6}$	$8.61 \times 10^{-7}$	2.414	0.015764 *
Area of shrubland	$3.84 \times 10^{-7}$	$8.51 \times 10^{-8}$	4.51	$6.49 \times 10^{-6}$ ***
Distance from road	$-3.06 \times 10^{-6}$	$1.73 \times 10^{-5}$	−0.177	0.859502

Null deviance: 3965.54 on 620 degrees of freedom. Residual deviance: 926.22 on 601 degrees of freedom. AIC: 1612.8. Number of Fisher scoring iterations: 6. Significance codes: 0, '\*\*\*' 0.001, '\*\*' 0.01, '\*' 0.05, '.' 0.1, ' ' 1.

Starting with the intercept, which represents the expected log of the mean landslide count when all other variables are zero, we found it to be highly significant ( $-5.249$ ,  $p < 2 \times 10^{-16}$ ). Among the continuous variables, we observed significant associations between landslide count and several factors. Curvature did not significantly affect landslide count ( $p = 0.248151$ ). Elevation, as represented via the DEM (digital elevation model), had a positive coefficient ( $0.00132$ ,  $p < 5.08 \times 10^{-12}$ ), suggesting that higher elevations are associated with increased landslide counts. This is understandable since steep slopes at higher elevations are more prone to slope instability and, thus, landslides.

Similarly, rainfall ( $0.001463$ ,  $p < 7.63 \times 10^{-13}$ ) was positively correlated with landslide count, implying that regions with higher rainfall tend to experience more landslides. Lineament was an important variable in our analysis, and it exhibited a significant negative coefficient ( $-0.5829$ ,  $p < 6.91 \times 10^{-12}$ ). This suggests that areas with a higher density of lineaments are associated with a lower incidence of landslides. Furthermore, relief ( $0.006422$ ,  $p < 0.000889$ ) positively affected the landslide count. Conversely, slope ( $-0.0001088$ ,  $p < 1.07 \times 10^{-8}$ ) had a negative coefficient, indicating that steeper slopes tend to have fewer landslides. This finding suggests that beyond a certain threshold, highly steep slopes may not provide the conditions necessary for landslides to occur.

For the categorical variable, namely geology, we included four categories: lower Siwalik, middle Siwalik, upper Siwalik, and quaternary. Middle Siwalik ( $-0.5935$ ,  $p < 2 \times 10^{-16}$ ) and upper Siwalik ( $-1.201$ ,  $p < 2 \times 10^{-16}$ ) both had negative coefficients, indicating that these geological formations were associated with lower landslide counts compared to lower Siwalik ones. Quaternary ( $-1.322$ ,  $p < 6.87 \times 10^{-7}$ ) also had a negative coefficient, implying a similar trend.

Additionally, several other variables were significant predictors of landslide count. Solar radiation ( $2.007 \times 10^{-2}$ ,  $p < 7.44 \times 10^{-13}$ ) had a positive effect, implying that areas

with higher solar radiation levels experience more landslides. This could be attributed to the influence of solar radiation on soil moisture, vegetation growth, and erosion processes, which, in turn, affect landslide activity. The area under water ( $1.239 \times 10^{-6}$ ,  $p = 0.009679$ ) showed a negative coefficient, suggesting that the presence of water bodies might decrease landslide counts. Several land cover types were also found to be significant predictors of landslide count. The areas under forest ( $2.73 \times 10^{-7}$ ,  $p < 2 \times 10^{-16}$ ), grassland ( $2.207 \times 10^{-5}$ ,  $p < 1.36 \times 10^{-5}$ ), agricultural land ( $6.629 \times 10^{-7}$ ,  $p = 0.005454$ ), bare ground ( $2.079 \times 10^{-6}$ ,  $p = 0.015764$ ), and shrubland ( $3.836 \times 10^{-7}$ ,  $p < 6.49 \times 10^{-6}$ ) all had positive coefficients, suggesting that larger areas covered by forests, grasslands, agricultural land, bare ground, and shrubland positively influence landslide counts. Lastly, the distance to roads did not significantly affect the landslide count ( $p = 0.859502$ ). This indicates that the distance to roads may not significantly influence landslide activity in the study area.

The model fit was assessed using the deviance statistic. The substantial reduction in the residual deviance (from 3965.54 to 926.22) indicates that the included variables explain a considerable portion of the variation in landslide counts. This suggests that the model effectively captures the relationship between the predictors and landslide occurrence. The low AIC value (1612.8) further supports the adequacy of the model fit, indicating its ability to balance goodness-of-fit and model complexity.

#### 4.3. Landslide Susceptible Map

Utilizing the modeling above result, we delineated the landslide susceptibility map of the region in ArcGIS using the raster calculator toolkit, and this tool was further categorized into five categories using the built-in Jenks natural breaks classification (Figure 6). It showed that around 16%, or 414 km<sup>2</sup>, area of the Chure region of Dang and Surkhet district falls in the very-high-susceptibility zone; about 69%, or 1793 km<sup>2</sup>, area lies in the high-susceptibility zone; 12%, or 313 km<sup>2</sup>, area lies in the moderate-susceptibility zone; 2%, or 58 km<sup>2</sup>, area lies in the low-susceptibility zone, and 0.03%, or 1 km<sup>2</sup>, area lies in the very-low-susceptibility zone (Table 3). Overall, the Chure region of Dang is more vulnerable, with about 23% of the area having very high susceptibility compared to around 5% in the Surkhet district.

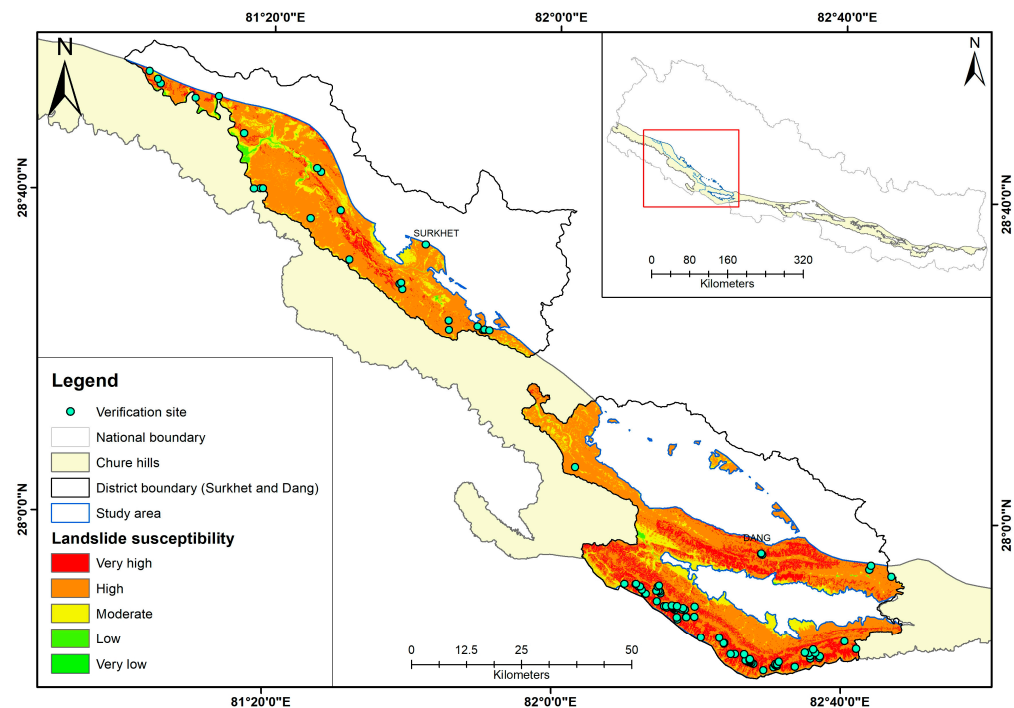


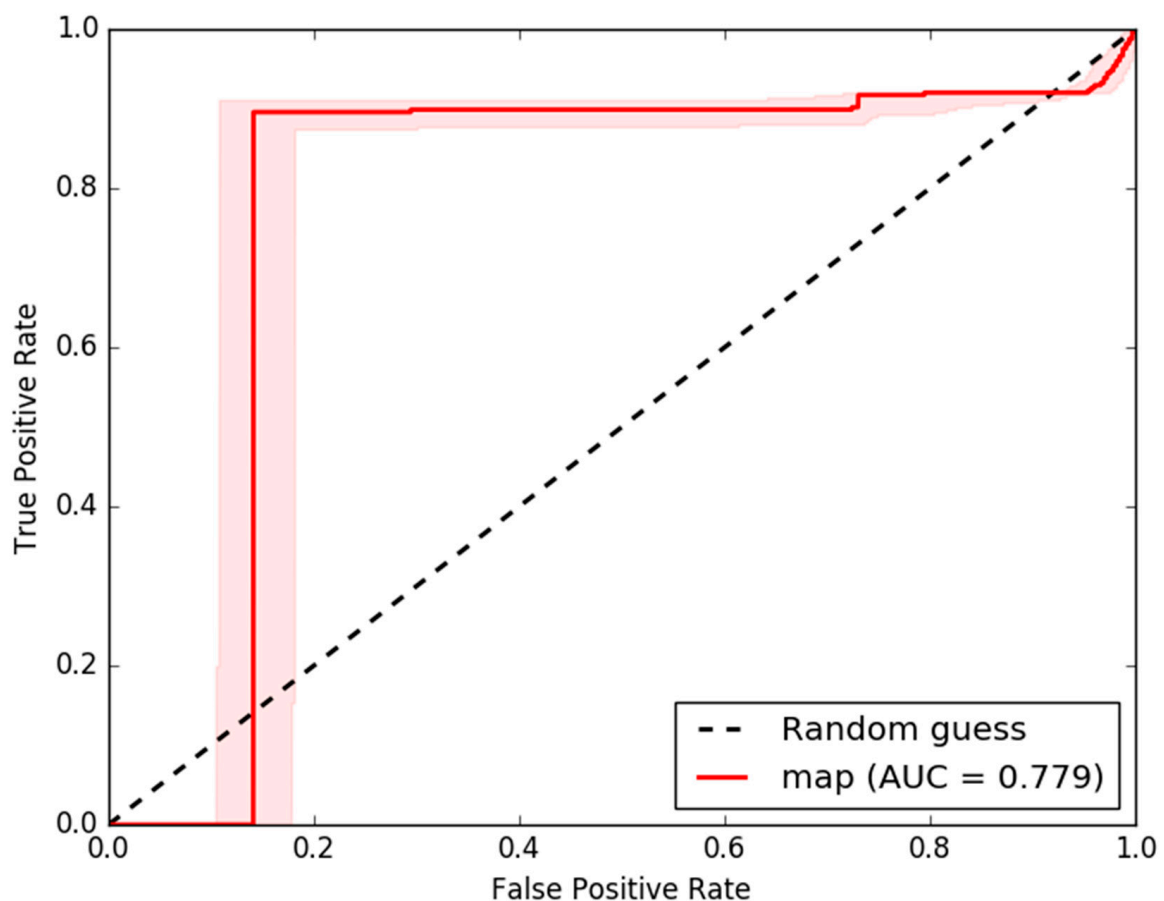
Figure 6. Landslide susceptibility map.

**Table 3.** The areas of Dang and Surkhet are located in different categories of the susceptibility map.

Risk Zone	Dang (km <sup>2</sup> )	Surkhet (km <sup>2</sup> )	Total
Very high	360 (23.32%)	54 (5.22%)	414 (16.05%)
High	994 (64.38%)	799 (77.20%)	1793 (69.52%)
Moderate	159 (10.30%)	154 (14.88%)	313 (12.14%)
Low	31 (2.01%)	27 (2.61%)	58 (2.25%)
Very low	0	1 (0.1%)	1 (0.04%)
<b>Total (km<sup>2</sup>)</b>	<b>1544</b>	<b>1035</b>	<b>2579</b>

#### 4.4. Validation

The validation was carried out for both the landslide points and the produced map. Due to resource constraints, only around 10% ( $n = 124$ ) of the randomly selected landslide points were verified in the field. From the field verification, we found that around 72% ( $n = 89$ ) of the landslides represented accurate landslide occurrences, and 28% might have been falsely identified as landslides. Furthermore, the produced landslide hazard map was validated through the ROC/AUC curve. The validation was conducted using the ArcSDM tool kit in ArcGIS, utilizing about 30% of the landslide points. The produced AUC value for the map was 0.779, which shows that the results are accurate (Figure 7).

**Figure 7.** ROC-AUC curve for the landslide susceptibility map.

## 5. Discussion

The main objective of this study was to assess landslide susceptibility in the highly vulnerable districts of the fragile Chure region using Poisson regression modeling. Previous studies have highlighted the geological fragility of the Chure region for landslides, and our findings are consistent with this trend. We observed a higher frequency of landslides

in the middle Siwalik, which aligns with the study by Bhandari and Dhakal [72] in the Babai Khola watershed. However, our modeling results suggest that lower Siwaliks are more susceptible to landslides. This could be due to the presence of a thicker weathered mudstone layer in the lower Siwalik, making it highly vulnerable to erosion-induced landslides [73].

Moreover, improper drainage management and the likelihood of floods in the lower Siwaliks [74,75] could exacerbate landslides and mass movement in this region. Another significant variable in our analysis was lineament density. The negative relationship indicates that higher lineament density reduces landslide susceptibility in this region. This finding contradicts the results of Lee and Talib [44], who conducted a factor analysis of landslides in Malaysia. Generally, higher lineament density is associated with more faults and fractures, weakening geology through weathering and erosion, especially during rainfall, when fractures induce soil movement [76,77]. However, in the case of our study area, the negative relationship means that a lower density of lineament is associated with a higher risk of landslides. According to Saha & Saha [78], areas with lineament density above  $1.5 \text{ km/km}^2$  are highly susceptible to landslides, but in our study area, almost 81% of the total areas were below the  $1.5 \text{ km/km}^2$  range.

The topographical variables found to be significant were elevation, relief, and slope. In our study, elevation was found to positively affect landslides. This can be attributed to various anthropogenic activities, such as development and agriculture, along the fragile and sloping regions at higher elevations, as Gurung et al. [79] reported in the Indrawati watershed of Nepal. Similarly, relief and slope were also found to be significant factors causing landslides, which is in line with the results of Ghimire [80], who reported slope and relief as proxy indicators for landslide susceptibility mapping in the Siwalik region. Furthermore, our study suggests that the probability of landslide occurrence in the Chure region decreases as the slope increases. Similar findings have been reported by Devkota et al. [41] in the Mugling–Narayanghat road section of Nepal and Regmi and Poudel [42] in the Patlu Khola watershed in Dang. This characteristic nature of landslides might have been observed due to fewer anthropogenic activities occurring on higher slopes, which can cause slope failure [79].

Among the three climatic variables, rainfall and solar radiation were significant in our modeling results. We observed a positive relationship between rainfall and landslide occurrence, suggesting that higher amounts of precipitation increase the risk of landslides. This finding is in congruence with the study by Petley et al. [3], which reported a strong correlation between the monsoon season and landslides in Nepal. Furthermore, solar radiation was found to have a positive relationship with and be an important predictor of regional landslides. Similar positive relationships between solar radiation and landslide occurrences have been reported by Cheng et al. [81] in their landslide prediction study conducted in Taiwan. The impact of solar radiation on landslides is similar to that of aspect, as described by Du et al. [82], where southern aspects receiving higher sunlight are more vulnerable to landslides [83]. The relationship between landslides and solar radiation can also be explained by the fact that areas with higher solar exposure tend to have less moisture and sparse vegetation, making them more susceptible to landslides [82,84].

Despite very low estimates, we found that areas under forest, shrubland, grassland, agricultural land, and bare ground were significant and positively related to landslides. Various studies have also reported the outburst of and debris flow from water bodies like rivers, streams, and waterfalls, which are severe problems for landslides [85,86]. Similarly, increasing unsustainable agricultural activities and unmanaged development activities have also been reported by Alimohammadlou et al. [87] as major triggering agents for landslides. Contrastingly, vegetation areas like forests have been reported as insignificant variables in various studies worldwide [88,89]. The significant result in our case may be due to the less productive land of the Chure region, resulting in a struggle for vegetation growth and low stem volume per ha, along with the middle mountains [7]. Hence, restrictions have been implemented in green felling to reduce the vulnerability of the Chure region.

Furthermore, indicative growing stock increments for the Chure region have been limited to 1% in forest management plans, out of which only 40% is allowed to be harvested in the community forests of the Chure region of Nepal to minimize ecological degradation [90]. Similar actions and policies enforced in the region further support our results, as even forests and other vegetative areas are prone to landslides in the Chure region.

We created a susceptibility map from the modeling results with five categories: very high, high, moderate, low, and very low. Our findings indicate that most of the study area falls into the very-high- (16%) and high (69%)-susceptibility categories, highlighting the high vulnerability of the Chure region in the Dang and Surkhet districts. These results align with the findings of Gyawali and Tamrakar [86], whose landslide susceptibility assessment of the Chure Khola catchment area reported around 72.46% of their study area to be in the very-high- and high-susceptibility categories.

To assess the accuracy of our susceptibility map, we employed the area under curve (AUC) technique and obtained a value of 0.779 (77.9%). This indicates that our final susceptibility map has accurate results and is consistent with other studies that used different techniques in Nepal. For example, Dahal et al. [91] utilized a weight of evidence modeling approach in the Lesser Himalaya range of the Kathmandu Valley and achieved a prediction rate of 79%. Similarly, Gyawali and Tamrakar [92] reported a 78% accuracy using their statistical index method. We recommend incorporating land cover changes into the modeling process to further improve the model and its accuracy. Dynamic land cover data can provide valuable insights regarding the changes in vegetation, urbanization, and other land-use practices that may influence landslide occurrences over time. By considering these temporal changes, the model can be better calibrated and adapted to the evolving landscape of the Chure region.

Our analysis observed an insignificant relationship between the distance to roads and landslide counts. This finding is consistent with the study conducted by Thapa and Bhandari [35], which also reported a weak relationship between road networks and landslide susceptibility in the Siwalik region. In contrast, we found that geology, climatic, and topographical variables had higher influences on landslide susceptibility in our study. The region's high percentage of landslide-susceptible areas underscores the need to carefully consider developmental activities and anthropogenic projects, such as sand mining, in the Chure region. It is essential for such projects to undergo a comprehensive environmental impact assessment (EIA) before their commencement.

## 6. Conclusions

Our comprehensive Poisson regression analysis of landslide occurrences in the sandy Chure region revealed significant insights regarding the relationships between various environmental variables and landslide counts. The results highlighted the significance of geology, lineament density, elevation, relief, slope, solar radiation, and land cover types as crucial predictors of landslide counts. Higher elevations and increased rainfall were positively correlated with landslide counts, while lineament density and slope exhibited negative relationships. Relief and solar radiation had positive effects, indicating that areas with higher relief and solar exposure experienced more landslides. The categorical variable, namely geology, highlighted lower landslide counts in middle Siwalik, upper Siwalik, and Quaternary geological formations compared to lower Siwalik. The distance to the road did not significantly affect landslide counts. The developed landslide susceptibility map identified high-susceptibility areas in the Chure hills of the Dang and Surkhet districts, emphasizing the urgent need for disaster mitigation measures and responsible land-use planning. Dang, in particular, was identified as more vulnerable, with about 23% of the area falling into the very-high-susceptibility zone, compared to around 5% in Surkhet. The robustness of our model, which is supported by a 77.9% accuracy rate in the AUC analysis, solidifies the reliability of our findings. Overall, this study provides valuable insights into the factors influencing landslide occurrences in the Chure region, and the developed

susceptibility map can serve as a valuable tool for decision-makers for prioritizing risk management efforts and enhancing disaster preparedness in the study area.

**Author Contributions:** P.B.T., Conceptualization, data, materials and funding acquisition; S.L., conceptualization, methodology, data curation and writing-original draft preparation, supervision, review and editing; K.P.J., conceptualization, methodology, data curation, writing-original draft preparation, review and editing; A.R.R., conceptualization, writing-original draft preparation, review and editing; D.B., conceptualization, writing-original draft preparation, review and editing; H.A., supervision, review and editing, funding acquisition. All authors have read and agreed to the published version of the manuscript.

**Funding:** This research received no external funding.

**Data Availability Statement:** The data presented in this study are available on request from the corresponding author.

**Conflicts of Interest:** The authors declare no conflict of interest.

## References

1. Highland, L. *Estimating Landslide Losses—Preliminary Results of a Seven-State Pilot Project*; US Geological Survey Reston: Reston, VA, USA, 2006.
2. Kjekstad, O.; Highland, L. Economic and Social Impacts of Landslides. In *Landslides—Disaster Risk Reduction*; Sassa, K., Canuti, P., Eds.; Springer: Berlin/Heidelberg, Germany, 2009; pp. 573–587. ISBN 978-3-540-69970-5.
3. Petley, D.N.; Hearn, G.J.; Hart, A.; Rosser, N.J.; Dunning, S.A.; Owen, K.; Mitchell, W.A. Trends in Landslide Occurrence in Nepal. *Nat. Hazards* **2007**, *43*, 23–44. [[CrossRef](#)]
4. Upreti, B.N. The Physiography and Geology of Nepal and Their Bearing on the Landslide Problem. In *Landslide Hazard Mitigation in the Hindu Kush-Himalaya*; International Centre for Integrated Mountain Development: Kathmandu, Nepal, 2001; pp. 31–49.
5. Subedi, B.; Lamichhane, P.; Magar, L.K.; Subedi, T. Aboveground Carbon Stocks and Sequestration Rates of Forests under Different Management Regimes in Churia Region of Nepal. *Banko Janakari* **2022**, *32*, 15–24. [[CrossRef](#)]
6. Singh, B.K. Land Tenure and Conservation in Chure. *J. For. Livelihood* **2017**, *15*, 87–102. [[CrossRef](#)]
7. Department of Forest Research and Survey. *State of Nepal's Forests*; Department of Forest Research and Survey: Kathmandu, Nepal, 2014.
8. Chaudhary, R.; Subedi, C. Chure-Tarai Madhesh Landscape, Nepal from Biodiversity Research Perspective. *Plant Arch.* **2019**, *19*, 351–359.
9. PCTMCD. *President Chure-Tarai Madhesh Conservation and Management Master Plan*; President Chure-Tarai Madhesh Conservation Development Board: Lalitpur, Nepal, 2018.
10. Alharbi, T.; Sultan, M.; Sefry, S.; ElKadiri, R.; Ahmed, M.; Chase, R.; Milewski, A.; Abu Abdullah, M.; Emil, M.; Chounaird, K. An Assessment of Landslide Susceptibility in the Faifa Area, Saudi Arabia, Using Remote Sensing and GIS Techniques. *Nat. Hazards Earth Syst. Sci.* **2014**, *14*, 1553–1564. [[CrossRef](#)]
11. Nhu, V.-H.; Mohammadi, A.; Shahabi, H.; Ahmad, B.B.; Al-Ansari, N.; Shirzadi, A.; Clague, J.J.; Jaafari, A.; Chen, W.; Nguyen, H. Landslide Susceptibility Mapping Using Machine Learning Algorithms and Remote Sensing Data in a Tropical Environment. *Int. J. Environ. Res. Public Health* **2020**, *17*, 4933. [[CrossRef](#)]
12. Ullah, I.; Aslam, B.; Shah, S.H.I.A.; Tariq, A.; Qin, S.; Majeed, M.; Havenith, H.-B. An Integrated Approach of Machine Learning, Remote Sensing, and GIS Data for the Landslide Susceptibility Mapping. *Land* **2022**, *11*, 1265. [[CrossRef](#)]
13. Shi, X.; Liao, M.; Zhang, L.; Balz, T. Landslide Stability Evaluation Using High-Resolution Satellite SAR Data in the Three Gorges Area. *Q. J. Eng. Geol. Hydrogeol.* **2016**, *49*, 203–211. [[CrossRef](#)]
14. Van Westen, C.J.; Rengers, N.; Soeters, R. Use of Geomorphological Information in Indirect Landslide Susceptibility Assessment. *Nat. Hazards* **2003**, *30*, 399–419. [[CrossRef](#)]
15. Saleem, N.; Huq, M.E.; Twumasi, N.Y.D.; Javed, A.; Sajjad, A. Parameters Derived from and/or Used with Digital Elevation Models (DEMs) for Landslide Susceptibility Mapping and Landslide Risk Assessment: A Review. *ISPRS Int. J. Geo-Inf.* **2019**, *8*, 545. [[CrossRef](#)]
16. Zhao, C.; Lu, Z. Remote Sensing of Landslides—A Review. *Remote Sens.* **2018**, *10*, 279. [[CrossRef](#)]
17. Corominas, J.; van Westen, C.; Frattini, P.; Cascini, L.; Malet, J.-P.; Fotopoulou, S.; Catani, F.; Van Den Eeckhaut, M.; Mavrouli, O.; Agliardi, F.; et al. Recommendations for the Quantitative Analysis of Landslide Risk. *Bull. Eng. Geol. Environ.* **2014**, *73*, 209–263. [[CrossRef](#)]
18. Ghimire, M.; Timalisina, N. Landslide Distribution and Processes in the Hills of Central Nepal: Geomorphic and Statistical Approach to Susceptibility Assessment. *J. Geosci. Environ. Prot.* **2020**, *8*, 276–302. [[CrossRef](#)]
19. Kanungo, D.P.; Arora, M.K.; Sarkar, S.; Gupta, R.P. A Comparative Study of Conventional, ANN Black Box, Fuzzy and Combined Neural and Fuzzy Weighting Procedures for Landslide Susceptibility Zonation in Darjeeling Himalayas. *Eng. Geol.* **2006**, *85*, 347–366. [[CrossRef](#)]

20. Raghuvanshi, T.K.; Ibrahim, J.; Ayalew, D. Slope Stability Susceptibility Evaluation Parameter (SSEP) Rating Scheme—an Approach for Landslide Hazard Zonation. *J. Afr. Earth Sci.* **2014**, *99*, 595–612. [[CrossRef](#)]
21. Carrara, A.; Cardinali, M.; Guzzetti, F.; Reichenbach, P. Gis Technology in Mapping Landslide Hazard. In *Geographical Information Systems in Assessing Natural Hazards*; Carrara, A., Guzzetti, F., Eds.; Advances in Natural and Technological Hazards Research; Springer: Dordrecht, The Netherlands, 1995; pp. 135–175. ISBN 978-94-015-8404-3.
22. Safaei, M.; Omar, H.; Huat, B.K.; Yousof, Z.B.; Ghiasi, V. Deterministic Rainfall Induced Landslide Approaches, Advantage and Limitation. *Electron. J. Geotech. Eng.* **2011**, *16*, 1619–1650.
23. Anis, Z.; Wissem, G.; Vali, V.; Smida, H.; Essghaier, G.M. GIS-Based Landslide Susceptibility Mapping Using Bivariate Statistical Methods in North-Western Tunisia. *Open Geosci.* **2019**, *11*, 708–726. [[CrossRef](#)]
24. Pradhan, B.; Lee, S. Landslide Susceptibility Assessment and Factor Effect Analysis: Backpropagation Artificial Neural Networks and Their Comparison with Frequency Ratio and Bivariate Logistic Regression Modelling. *Environ. Model. Softw.* **2010**, *25*, 747–759. [[CrossRef](#)]
25. Abdo, H.G. Assessment of Landslide Susceptibility Zonation Using Frequency Ratio and Statistical Index: A Case Study of Al-Fawar Basin, Tartous, Syria. *Int. J. Environ. Sci. Technol.* **2022**, *19*, 2599–2618. [[CrossRef](#)]
26. Mersha, T.; Meten, M. GIS-Based Landslide Susceptibility Mapping and Assessment Using Bivariate Statistical Methods in Simada Area, Northwestern Ethiopia. *Geoenviron Disasters* **2020**, *7*, 20. [[CrossRef](#)]
27. Guo, M.; Li, J.; Sheng, C.; Xu, J.; Wu, L. A Review of Wetland Remote Sensing. *Sensors* **2017**, *17*, 777. [[CrossRef](#)] [[PubMed](#)]
28. Abija, F.A.; Nwosu, J.I.; Ifedotun, A.I.; Osadebe, C.C. Landslide Susceptibility Assessment of Calabar, Nigeria Using Geotechnical, Remote Sensing and Multi-Criteria Decision Analysis: Implications for Urban Planning and Development. *SDRP-JESES* **2019**, *4*, 774–788. [[CrossRef](#)]
29. Brenning, A. Spatial Prediction Models for Landslide Hazards: Review, Comparison and Evaluation. *Nat. Hazards Earth Syst. Sci.* **2005**, *5*, 853–862. [[CrossRef](#)]
30. Atkinson, P.M.; Massari, R. Generalised Linear Modelling of Susceptibility to Landsliding in the Central Apennines, Italy. *Comput. Geosci.* **1998**, *24*, 373–385. [[CrossRef](#)]
31. Crovelli, R.A. *Probability Models for Estimation of Number and Costs of Landslides*; US Geological Survey: Reston, VA, USA, 2000.
32. Das, I.; Kumar, G.; Stein, A.; Bagchi, A.; Dadhwal, V.K. Stochastic Landslide Vulnerability Modeling in Space and Time in a Part of the Northern Himalayas, India. *Environ. Monit. Assess* **2011**, *178*, 25–37. [[CrossRef](#)] [[PubMed](#)]
33. Chung, C.-J.F.; Fabbri, A.G.; Van Westen, C.J. Multivariate Regression Analysis for Landslide Hazard Zonation. In *Geographical Information Systems in Assessing Natural Hazards*; Carrara, A., Guzzetti, F., Eds.; Advances in Natural and Technological Hazards Research; Springer: Dordrecht, The Netherlands, 1995; pp. 107–133. ISBN 978-94-015-8404-3.
34. Shrestha, K.; Khadka, U.R.; Singh Shrestha, M. Comparative GIS-Based Assessment of Landslide Susceptibility of Chepe River Corridor, Gandaki River Basin, Nepal. In *Integrated Research on Disaster Risks*; Djalante, R., Bisri, M.B.F., Shaw, R., Eds.; Disaster Risk Reduction; Springer International Publishing: Berlin/Heidelberg, Germany, 2021; pp. 111–136. ISBN 978-3-030-55562-7.
35. Thapa, D.; Bhandari, B.P. GIS-Based Frequency Ratio Method for Identification of Potential Landslide Susceptible Area in the Siwalik Zone of Chatara-Barahakshetra Section, Nepal. *Open J. Geol.* **2019**, *09*, 873. [[CrossRef](#)]
36. CBS. *National Population and Housing Census 2021*; Central Bureau of Statistics: Kathmandu, Nepal; National Planning Commission: Kathmandu, Nepal, 2021.
37. Uprety, Y.; Tiwari, A.; Karki, S.; Chaudhary, A.; Yadav, R.K.P.; Giri, S.; Shrestha, S.; Paudyal, K.; Dhakal, M. Characterization of Forest Ecosystems in the Chure (Siwalik Hills) Landscape of Nepal Himalaya and Their Conservation Need. *Forests* **2023**, *14*, 100. [[CrossRef](#)]
38. Manandhar, E.; Kharel, B.P.; Basnet, L. Integrated River System Resource Management Planning: A Stepping Stone for Sustainable Conservation of Chure-TaraiMadhesh Landscape. In *Proceedings of the Seminar on Leaving no One Behind*; National Academy of Science and Technology: Khumaltar, Lalitpur, 12 October 2019.
39. Ghimire, M. Historical Land Covers Change in the Chure-Tarai Landscape in the Last Six Decades: Drivers and Environmental Consequences. In *Land Cover Change and Its Eco-Environmental Responses in Nepal*; Li, A., Deng, W., Zhao, W., Eds.; Springer Geography; Springer: Singapore, 2017; pp. 109–147. ISBN 978-981-10-2890-8.
40. Pourghasemi, H.R.; Kornejady, A.; Kerle, N.; Shabani, F. Investigating the Effects of Different Landslide Positioning Techniques, Landslide Partitioning Approaches, and Presence-Absence Balances on Landslide Susceptibility Mapping. *CATENA* **2020**, *187*, 104364. [[CrossRef](#)]
41. Devkota, K.C.; Regmi, A.D.; Pourghasemi, H.R.; Yoshida, K.; Pradhan, B.; Ryu, I.C.; Dhital, M.R.; Althuwaynee, O.F. Landslide Susceptibility Mapping Using Certainty Factor, Index of Entropy and Logistic Regression Models in GIS and Their Comparison at Mugling–Narayanghat Road Section in Nepal Himalaya. *Nat. Hazards* **2013**, *65*, 135–165. [[CrossRef](#)]
42. Regmi, A.D.; Poudel, K. Assessment of Landslide Susceptibility Using GIS-Based Evidential Belief Function in Patu Khola Watershed, Dang, Nepal. *Environ. Earth Sci.* **2016**, *75*, 743. [[CrossRef](#)]
43. Addis, A. GIS-Based Landslide Susceptibility Mapping Using Frequency Ratio and Shannon Entropy Models in Dejen District, Northwestern Ethiopia. *J. Eng.* **2023**, *2023*, e1062388. [[CrossRef](#)]
44. Lee, S.; Talib, J.A. Probabilistic Landslide Susceptibility and Factor Effect Analysis. *Environ. Geol.* **2005**, *47*, 982–990. [[CrossRef](#)]
45. He, S.; Pan, P.; Dai, L.; Wang, H.; Liu, J. Application of Kernel-Based Fisher Discriminant Analysis to Map Landslide Susceptibility in the Qinggan River Delta, Three Gorges, China. *Geomorphology* **2012**, *171–172*, 30–41. [[CrossRef](#)]

46. Shu, H.; Guo, Z.; Qi, S.; Song, D.; Pourghasemi, H.R.; Ma, J. Integrating Landslide Typology with Weighted Frequency Ratio Model for Landslide Susceptibility Mapping: A Case Study from Lanzhou City of Northwestern China. *Remote Sens.* **2021**, *13*, 3623. [CrossRef]
47. Ali, S.A.; Parvin, F.; Vojteková, J.; Costache, R.; Linh, N.T.T.; Pham, Q.B.; Vojtek, M.; Gigović, L.; Ahmad, A.; Ghorbani, M.A. GIS-Based Landslide Susceptibility Modeling: A Comparison between Fuzzy Multi-Criteria and Machine Learning Algorithms. *Geosci. Front.* **2021**, *12*, 857–876. [CrossRef]
48. Pham, B.T.; Bui, D.T.; Dholakia, M.B.; Prakash, I.; Pham, H.V.; Mehmood, K.; Le, H.Q. A Novel Ensemble Classifier of Rotation Forest and Naïve Bayer for Landslide Susceptibility Assessment at the Luc Yen District, Yen Bai Province (Viet Nam) Using GIS. *Geomat. Nat. Hazards Risk* **2017**, *8*, 649–671. [CrossRef]
49. Xu, C.; Dai, F.; Xu, X.; Lee, Y.H. GIS-Based Support Vector Machine Modeling of Earthquake-Triggered Landslide Susceptibility in the Jianjiang River Watershed, China. *Geomorphology* **2012**, *145–146*, 70–80. [CrossRef]
50. Clubb, F.J.; Mudd, S.M.; Attal, M.; Milodowski, D.T.; Grieve, S.W.D. The Relationship between Drainage Density, Erosion Rate, and Hilltop Curvature: Implications for Sediment Transport Processes. *J. Geophys. Res. Earth Surf.* **2016**, *121*, 1724–1745. [CrossRef]
51. Ding, Q.; Chen, W.; Hong, H. Application of Frequency Ratio, Weights of Evidence and Evidential Belief Function Models in Landslide Susceptibility Mapping. *Geocarto Int.* **2017**, *32*, 619–639. [CrossRef]
52. Moosavi, V.; Niazi, Y. Development of Hybrid Wavelet Packet-Statistical Models (WP-SM) for Landslide Susceptibility Mapping. *Landslides* **2016**, *13*, 97–114. [CrossRef]
53. Shirzadi, A.; Chapi, K.; Shahabi, H.; Solaimani, K.; Kaviani, A.; Ahmad, B.B. Rock Fall Susceptibility Assessment along a Mountainous Road: An Evaluation of Bivariate Statistic, Analytical Hierarchy Process and Frequency Ratio. *Environ. Earth Sci.* **2017**, *76*, 152. [CrossRef]
54. Henriques, C.; Zêzere, J.L.; Marques, F. The Role of the Lithological Setting on the Landslide Pattern and Distribution. *Eng. Geol.* **2015**, *189*, 17–31. [CrossRef]
55. Kim, K.-S.; Song, Y.-S. Geometrical and Geotechnical Characteristics of Landslides in Korea under Various Geological Conditions. *J. Mt. Sci.* **2015**, *12*, 1267–1280. [CrossRef]
56. Guzzetti, F.; Peruccacci, S.; Rossi, M.; Stark, C.P. Rainfall Thresholds for the Initiation of Landslides in Central and Southern Europe. *Meteorol. Atmos. Phys.* **2007**, *98*, 239–267. [CrossRef]
57. Hadji, R.; Chouabi, A.; Gadri, L.; Raïs, K.; Hamed, Y.; Boumazbour, A. Application of Linear Indexing Model and GIS Techniques for the Slope Movement Susceptibility Modeling in Bousselam Upstream Basin, Northeast Algeria. *Arab. J. Geosci.* **2016**, *9*, 192. [CrossRef]
58. Celtek, S. The Effect of Aspect on Landslide and Its Relationship with Other Parameters. In *Landslides*; IntechOpen: London, UK, 2021.
59. Singh, K.; Kumar, V. Hazard Assessment of Landslide Disaster Using Information Value Method and Analytical Hierarchy Process in Highly Tectonic Chamba Region in Bosom of Himalaya. *J. Mt. Sci.* **2018**, *15*, 808–824. [CrossRef]
60. Panchal, S.; Shrivastava, A.K. Landslide Hazard Assessment Using Analytic Hierarchy Process (AHP): A Case Study of National Highway 5 in India. *Ain. Shams Eng. J.* **2022**, *13*, 101626. [CrossRef]
61. R Core Team. *R: A Language and Environment for Statistical Computing*; R Foundation for Statistical Computing: Vienna, Austria, 2021.
62. LPDAAC. ASTER Global Digital Elevation Model V003 [Dataset]. NASA EOSDIS Land Processes Distributed Active Archive Center. 2019. Available online: <https://lpdaac.usgs.gov/products/astgtmv003/> (accessed on 18 October 2022).
63. Fick, S.E.; Hijmans, R.J. WorldClim 2: New 1 km spatial resolution climate surfaces for global land areas. *Int. J. Climatol.* **2017**, *27*, 4302–4315. [CrossRef]
64. ICIMOD. Geology of Nepal [Dataset]. 2020. Available online: <https://rds.icimod.org/home/datadetail?metadetail=2521> (accessed on 27 April 2022).
65. ESRI. Sentinel-2 10-Meter Land Use/Land Cover [Dataset]. 2020. Available online: <https://livingatlas.arcgis.com/landcover> (accessed on 22 May 2022).
66. OCHA Nepal. Nepal Road Network [Dataset]. Humanitarian Data Exchange. 2021. Available online: <https://data.humdata.org/dataset/nepal-road-network> (accessed on 18 October 2022).
67. Signorell, A.; Aho, K.; Alfons, A.; Anderegg, N.; Aragon, T.; Arppe, A.; Baddeley, A.; Barton, K.; Bolker, B.; Borchers, H.W. *DescTools: Tools for Descriptive Statistics*; R Package Version 0.99; R Project: Vienna, Austria, 2018; Volume 28, p. 17.
68. Racine, J.S. Rstudio: A Platform-Independent Ide for R and Sweave. *J. Appl. Econom.* **2012**, *27*, 167–172. [CrossRef]
69. Boomsma, A. Regression Diagnostics with R. In *Department of Statistics & Measurement Theory*; University of Groningen: Groningen, The Netherlands, 2014.
70. Chatterjee, S.; Hadi, A.S. Regression Diagnostics: Detection of Model Violations. In *Regression Analysis by Example*; John Wiley & Sons, Ltd.: Hoboken, NJ, USA, 2015; pp. 85–120. ISBN 978-0-470-05546-5.
71. Hosmer, D.W., Jr. Model-Building Strategies and Methods for Logistic Regression. *Appl. Logist. Regres.* **2013**, *22*, 89–151.
72. Bhandari, B.; Dhakal, S. Lithological Control on Landslide in the Babai Khola Watershed, Siwaliks Zone of Nepal. *Am. J. Earth Sci.* **2018**, *5*, 54–64.
73. Upreti, B.N. An Overview of the Stratigraphy and Tectonics of the Nepal Himalaya. *J. Asian Earth Sci.* **1999**, *17*, 577–606. [CrossRef]
74. Dhakal, S. Geological Divisions and Associated Hazards in Nepal. In *Contemporary Environmental Issues and Methods in Nepal*; Tribhuvan University: Kirtipur, Nepal, 2014; pp. 100–109.

75. McAdoo, B.G.; Quak, M.; Gnyawali, K.R.; Adhikari, B.R.; Devkota, S.; Rajbhandari, P.L.; Sudmeier-Rieux, K. Roads and Landslides in Nepal: How Development Affects Environmental Risk. *Nat. Hazards Earth Syst. Sci.* **2018**, *18*, 3203–3210. [[CrossRef](#)]
76. Lee, S. Geological Application of Geographic Information System. *Korea Inst. Geosci. Min. Resour.* **2014**, *9*, 109–118.
77. Ramli, M.F.; Yusof, N.; Yusoff, M.K.; Juahir, H.; Shafri, H.Z.M. Lineament Mapping and Its Application in Landslide Hazard Assessment: A Review. *Bull. Eng. Geol. Environ.* **2010**, *69*, 215–233. [[CrossRef](#)]
78. Saha, A.; Saha, S. Comparing the Efficiency of Weight of Evidence, Support Vector Machine and Their Ensemble Approaches in Landslide Susceptibility Modelling: A Study on Kurseong Region of Darjeeling Himalaya, India. *Remote Sens. Appl. Soc. Environ.* **2020**, *19*, 100323. [[CrossRef](#)]
79. Gurung, A.; Bista, R.; Karki, R.; Shrestha, S.; Uprety, D.; Oh, S.E. Community-Based Forest Management and Its Role in Improving Forest Conditions in Nepal. *Small-Scale For.* **2013**, *12*, 377–388. [[CrossRef](#)]
80. Ghimire, M. Landslide Occurrence and Its Relation with Terrain Factors in the Siwalik Hills, Nepal: Case Study of Susceptibility Assessment in Three Basins. *Nat. Hazards* **2011**, *56*, 299–320. [[CrossRef](#)]
81. Cheng, Y.-S.; Yu, T.-T.; Son, N.-T. Random Forests for Landslide Prediction in Tsengwen River Watershed, Central Taiwan. *Remote Sens.* **2021**, *13*, 199. [[CrossRef](#)]
82. Du, J.; Glade, T.; Woldai, T.; Chai, B.; Zeng, B. Landslide Susceptibility Assessment Based on an Incomplete Landslide Inventory in the Jilong Valley, Tibet, Chinese Himalayas. *Eng. Geol.* **2020**, *270*, 105572. [[CrossRef](#)]
83. Gautam, A.P.; Shivakoti, G.P.; Webb, E.L. A Review of Forest Policies, Institutions, and Changes in the Resource Condition in Nepal. *Int. For. Rev.* **2004**, *6*, 136–148. [[CrossRef](#)]
84. Måren, I.E.; Karki, S.; Prajapati, C.; Yadav, R.K.; Shrestha, B.B. Facing North or South: Does Slope Aspect Impact Forest Stand Characteristics and Soil Properties in a Semiarid Trans-Himalayan Valley? *J. Arid. Environ.* **2015**, *121*, 112–123. [[CrossRef](#)]
85. Kayastha, P.; Dhital, M.R.; De Smedt, F. Application of the Analytical Hierarchy Process (AHP) for Landslide Susceptibility Mapping: A Case Study from the Tinau Watershed, West Nepal. *Comput. Geosci.* **2013**, *52*, 398–408. [[CrossRef](#)]
86. Zekkos, D.; Clark, M.; Whitworth, M.; Greenwood, W.; West, A.J.; Roback, K.; Li, G.; Chamlagain, D.; Manousakis, J.; Quack-enbush, P.; et al. Observations of Landslides Caused by the April 2015 Gorkha, Nepal, Earthquake Based on Land, UAV, and Satellite Reconnaissance. *Earthq. Spectra* **2017**, *33*, 95–114. [[CrossRef](#)]
87. Alimohammadlou, Y.; Najafi, A.; Yalcin, A. Landslide Process and Impacts: A Proposed Classification Method. *Catena* **2013**, *104*, 219–232. [[CrossRef](#)]
88. Haigh, M.J.; Rawat, J.S.; Rawat, M.S.; Bartarya, S.K.; Rai, S.P. Interactions between Forest and Landslide Activity along New Highways in the Kumaun Himalaya. *For. Ecol. Manag.* **1995**, *78*, 173–189. [[CrossRef](#)]
89. Schmaltz, E.M.; Steger, S.; Glade, T. The Influence of Forest Cover on Landslide Occurrence Explored with Spatio-Temporal Information. *Geomorphology* **2017**, *290*, 250–264. [[CrossRef](#)]
90. Baral, S.; Vacik, H. What Governs Tree Harvesting in Community Forestry-Regulatory Instruments or Forest Bureaucrats' Discretion? *Forests* **2018**, *9*, 649. [[CrossRef](#)]
91. Dahal, R.K.; Hasegawa, S.; Bhandary, N.P.; Poudel, P.P.; Nonomura, A.; Yatabe, R. A Replication of Landslide Hazard Mapping at Catchment Scale. *Geomat. Nat. Hazards Risk* **2012**, *3*, 161–192. [[CrossRef](#)]
92. Gyawali, P.; Tamrakar, N.K. Landslide Susceptibility Assessment of the Chure Khola Catchment Area of the Siwalik Region, Central Nepal. *J. Nepal Geol. Soc.* **2018**, *56*, 19–30. [[CrossRef](#)]

**Disclaimer/Publisher's Note:** The statements, opinions and data contained in all publications are solely those of the individual author(s) and contributor(s) and not of MDPI and/or the editor(s). MDPI and/or the editor(s) disclaim responsibility for any injury to people or property resulting from any ideas, methods, instructions or products referred to in the content.